Presented at: 7th Advanced Accelerator Concepts Workshop
Lake Tahoe, CA
October 13-18, 1996

CONF-9610210--11

BNL- 63808

Commissioning Results of the Next Generation Photoinjector

D. T. Palmer*, X. J. Wang†, R. H. Miller*, M. Babzien†, I. Ben-Zvi†,
C. Pellegrini*, J. Sheehna†, J. Skaritka†, H. Winick*, M. Woodle†, V. Yakimenko†

*Stanford Linear Accelerator Center, Stanford University, Stanford, CA 94309
†Brookhaven National Laboratory, Accelerator Test Facility, Upton, NY 11973
*University of California Los Angles, Department of Physics, Los Angles, CA 90095

5910000
0936000
114000

December 1996

National Synchrotron Light Source
Brookhaven National Laboratory
Upton, NY 11973

Work performed under the auspices of the U.S. Department of Energy,
under contract DE-AC02-76CH00016

DISCLAIMER

Portions of this document may be illegible in electronic image products. Images are produced from the best available original document.

Commissioning Results of the Next Generation Photoinjector

D. T. Palmer*, X. J. Wang†, R. H. Miller*
M. Babzien†,I. Ben-Zvi†, C. Pellegrini*, J. Sheehna†,
J. Skaritka†, H. Winick*, M. Woodle†, V.Yakimenko†

*Stanford Linear Accelerator Center
Stanford University, Stanford CA 94309

†Brookhaven National Laboratory
Accelerator Test Facility
Upton, NY 11973

*University of California Los Angles
Department of Physics
Los Angles CA 90095

5910000 RECEIVED
FEB 06 1997
OSTI
0936000
1144000

Abstract

The Next Generation Photoinjector (NGP) developed by the BNL / SLAC / UCLA collaboration was installed at the Brookhaven National Laboratories Accelerator Test Facility (ATF). The commissioning results and performance of the photocathode injector are present. The Next Generation Photoinjector consists of the symmetrized BNL/SLAC/UCLA 1.6 cell S-band Photocathode RF gun and a single solenoidal magnet for transverse emittance compensation [1]. The highest acceleration field achieved on the cathode is 150 $\frac{MV}{m}$, and the RF guns normal operating field is 130 $\frac{MV}{m}$. The quantum efficiency of the copper cathode was measured to be 4.5×10^{-5}. The transverse emittance and bunch length of the photoelectron beam were measured. The optimized rms normalized emittance for a charge of 300 pC is 0.7 π mm mrad. The bunch length dependency of photoelectron beam on the RF gun phase and acceleration fields were experimentally investigated.

MASTER

DISTRIBUTION OF THIS DOCUMENT IS UNLIMITED

1 Introduction

The NGP has been installed at the ATF, as the electron source for beam dynamics studies, laser acceleration and free electron laser experiments. The injector consists of the symmetrized BNL/SLAC/UCLA 1.6 cell S-band Photocathode RF gun, powered by a XK-5 klystron, and a single emittance compensation solenoidal magnet. There is a short drift space between the NGP and the input to the first of two SLAC 3 meters travelling wave accelerating sections. This low energy drift space contains a copper mirror that can be used in either transition radiation studies or laser alignment. There is also a beam profile monitor/faraday plate located 66.4 cm from the cathode plane.

Two SLAC travelling wave linacs, are power from a single XK-5 klystron. The high energy beam transport system consists of nine quadrupole magnets, energy spectrometer, energy selection slit and high energy faraday cup. Diagnostics located in the high energy transport consist of beam profile monitors and strip lines. The strip lines are used for an on line laser/RF phase stability monitor.

The laser system consists of a diode pumped Nd:YAG oscillator. The Nd:YAG oscillator generated 81.6 MHz pulses with 21 ps FWHM pulse lengths and a 100 mW of average power. The seed pulse produced by the oscillator is imaged and amplified by two-stage Nd:YAG amplifiers. The IR is frequency quadrupled to UV (266 nm) on the laser table. This nonlinear process leads to a factor of two reduction in the laser pulse length. The beam is transported to the RF gun area via a 20 meter long evacuated pipe. The laser beam transport system near the injector includes an aperture, a set of telescoping lenses and a limiting aperture. This limiting aperture is imaged onto the cathode, by a pair of cylindrical lenses. The focal lengths and locations of these lenses were chosen to compensate for the ellipticity of the emitting area caused by oblique incidence. The time skew, also due to the lasers oblique incidence on the cathode, has been corrected for using a gradient. The relay imaging technique used throughout the optical transport improves the beam pointing stability. Since the laser beam overfills the limiting aperture, the transverse profile of the beam is nearly top hat. The spot size of the laser beam on the cathode is 2 mm diameter edge to edge.

2 Injector Design

The 1.6 cell RF gun differs from the original BNL 1.5 cell RF gun [2] in that the half cell has been lengthen to decrease the RF field levels on the cell to cell coupling iris and also to provide more RF focusing in the iris region. The 1.6 cell RF gun is not a side coupled 0-mode suppressed RF gun, as in the previous BNL type RF guns. High power RF is coupled into the full cell and the increased beam iris diameter increase the cell to cell coupling, which provides a mode separation of 3.225MHz for a balanced field configuration. The half

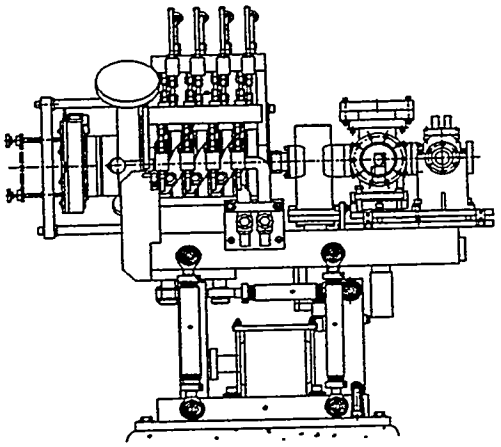

Figure 1: Next Generation Photoinjector

cell is fully symmetrized with two oblique incidence laser ports. The cathode plate is removable, using a helico flex seal for both the vacuum and RF seals. The removable cathode plate eliminates the multipacktering problem common to choke joint cathodes. The removable cathode allows for easy replacement of different cathode materials such as Cu and Mg. The Cu cathode results are presented in this paper. The full cell has two symmetrized plunger type tuners. The bandwidth of this pair of tuners is ± 2 MHz. The RF coupling slot is symmetrized by a identical coupling slot that provides additional vacuum pumping [3]. The 1.6 cell gun uses resistive heating versus water cooling to maintain the guns resonance frequency.

The single emittance compensation magnet, that was specifically designed to be used with the 1.6 cell gun, utilized POISSON [4] field maps into PARMELA [5] to study the beam dynamics consideration of different magnet designs. In previous emittance compensation system designs, a bucking coil is position downstream of the cathode plane. Magnetic field measurements of the magnetic field at the cathode are less than 9 gauss for the maximum solenoidal field of 3 Kg. Simulations indicate the magnetic emittance term scales as $0.01 \frac{\pi\ mm\ mrad}{gauss}$. Considering that constructing and alignment of an identical bucking magnet uses valuable space behind the cathode that can be used for other experimental devices, such as a load lock for UHV cathode replacement, it was decided that the an identical bucking magnet was not needed.

The 1.6 cell RF gun operates at $5\text{x}10^{-9}$ torr with a field gradient of 130 $\frac{MV}{m}$ and in the quiescent state the vacuum is 10^{-9} torr.

3 Gun Energy / Dark Current

The BNL/SLAC/UCLA 1.6 cell S-band Photocathode RF gun is designed to attain field level at the cathode and the middle of the full cell up to 150 $\frac{MeV}{m}$ and operate with RF pulse widths up to 3.5 μs. Calibration of the field levels in the gun were verified by measurements of the beam energy using a $\cos(\theta)$ deflec-

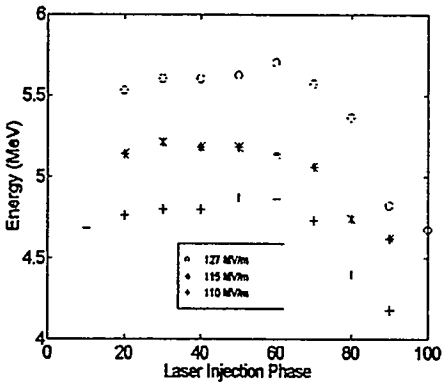

Figure 2: Energy versus Field Level

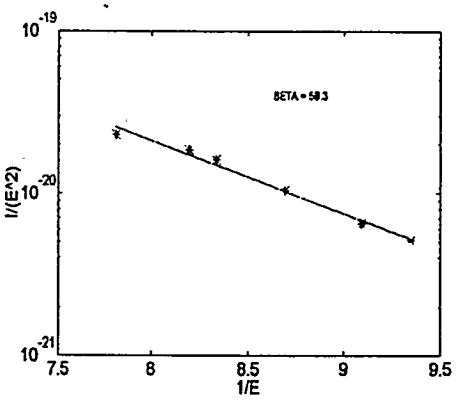

Figure 3: Fowler-Nordheim Plot

tion magnet located inside the bore of the emittance compensation solenoidal magnet. These energy measurements are shown in figure 2.

Standard machining and a Cu wool polishing techniques were used to manufacture both the full and half cells. The cathode plate was prepared using the procedures detailed in reference [6]. These techniques when combined together produce a field enhancement factor $\beta = 58$ as can be seen in the Fowler-Nordheim Plot of figure 3.

4 Multi-Pole Fields

Multi-pole field effects were studied by decreasing the laser spot size to 400 μm and setting the laser injection phase to the Schottky peak. This injection phase causes an effective electron bunch lengthening and a noticeable energy spread tail was observed. By adjusting the laser spot position we were able to eliminate this energy spread tail. This laser spot realignment minimizes the integrated higher order mode contribution to the beam distortion. Analysis indicate that the symmetrized BNL/SLAC/UCLA 1.6 cell Photocathode RF guns electrical and geometry center are within 170 μm of each other, which is within the laser spot alignment error of 250 μm. Compared to similar experimental results of the 1.5 cell BNL gun whose electrical and geometric centers differ by 1.0 mm [7], the 1.6 cell gun has fulfilled the symmeterization criteria. Future work with custom laser masks to study the field patterns at larger diameters are planned for the future [8].

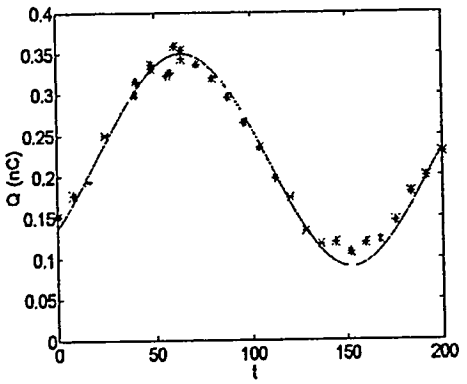

Figure 4: Electron Bunch Charge versus Polarizer Angle

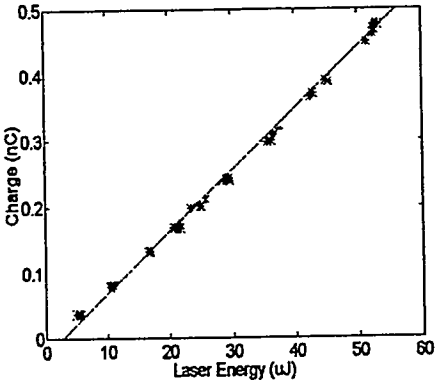

Figure 5: Electron Bunch Charge versus Laser Power

5 Quantum Efficiency versus Polarization

Time skew grating and cylindrical lens have been installed to correct for the lasers oblique incidence angle of 72°. Time skew correction has the draw back of decreasing the available laser energy at the cathode by 50%. The available charge was maximized by adjusting the lasers polarization. In figure 4 it can be seen that the available charge is maximized at a polarizer angle of 56° which correspondence to P-type polarized light on the cathode.

The measured value of the Cu cathode's quantum efficiency is QE = $4.5\text{x}10^{-5}$ which is calculated from figure 5. These studies were conducted at a laser injection phase of 90° which utilized the Schottky effect to increase the measured charge.

6 Transverse Phase Space

The normalized rms emittance, $\epsilon_{n,rms}$, measurements were taken using a variation of the three screen method. Two screens were utilized while insuring that at beam waist was located at the down stream profile screen. The two screen method is compared to standard quadrupole scan technique in figure 6 and the results from these two methods are compared in table 1

PARMELA was used to simulate the emittance compensation process and the subsequent acceleration to 40 MeV [9]. A correlation of the minimum spot size with an emittance minimum was noted during these simulations. This was experimentally verified during the commissioning of the 1.6 cell RF gun, using the beam profile monitor located at the output of the second linac section, as

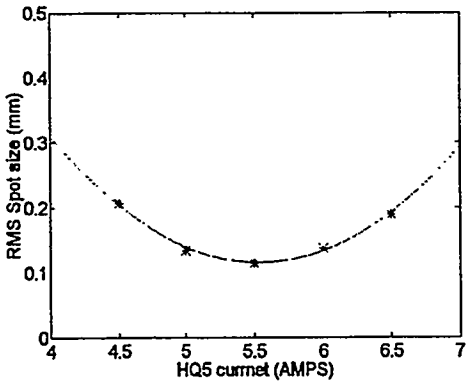

Figure 6: Quadrupole Scan RMS Emittance Results

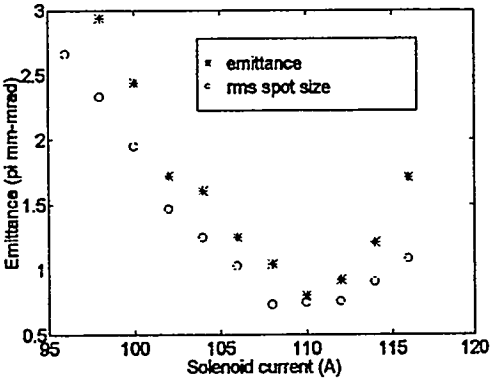

Figure 7: $\epsilon_{n,rms}$ and RMS Beam Size versus Solenoidal field

can be seen in figure 7. These results are consistent with similar results of the BNL 1.5 cell RF gun [7].

There are four emittance terms that contribute to the total $\epsilon_{n,rms}$ these are the ϵ_{sc}, ϵ_{rf}, $\epsilon_{thermal}$ and ϵ_{mag}. The last term is due to the small but finite magnetic field at the cathode.

Studying the dependence of transverse emittance on the bunch charge in figure 8, we have noted that there is a residual emittance term of 0.2 π mm mrad. This term is due to ϵ_{rf}, $\epsilon_{thermal}$, ϵ_{mag} and resolution error. If we neglect the magnetic term, which is reasonable due to the initial cathode spot size and the small magnetic field at the cathode we can estimate the thermal and RF emittance terms to be less than the 0.2 π mm mrad. Since the measured $\epsilon_{n,rms}$ is less than the ϵ_{sc} that Kim's theory [10] predicates by a factor of three we are confident that we have produced an emittance compensated beam.

Due to laser power limitation, RF gun bunch compression and the Schottky effect it is not possible to keep the peak current constant for different laser injection phases. Therefore in figure 9 the plot is not for a constant current but for a decreasing charge from a maximum of 400 pC to a minimum of 178 pC.

$\epsilon_{n,rms}$ Quad Scan	2.29 π mm-mrad
$\epsilon_{n,rms}$ Two Screen	2.42 π mm-mrad

Table 1: Quad Scan and Two Screen Method Results

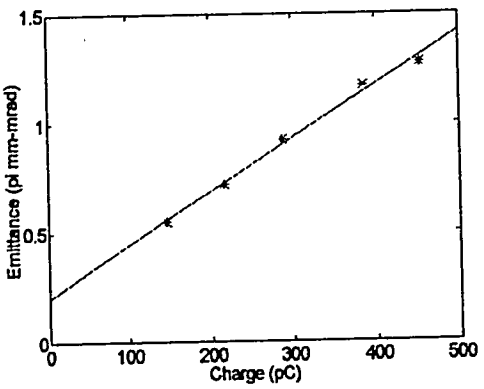

Figure 8: $\epsilon_{n,rms}$ versus Electron Bunch Charge

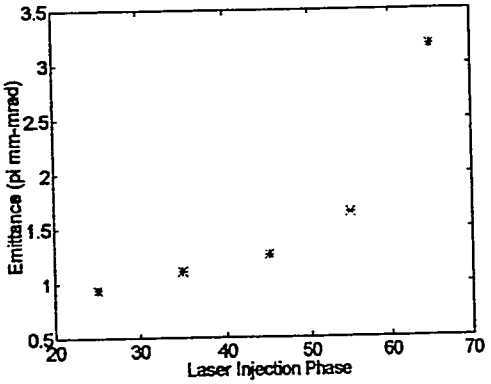

Figure 9: $\epsilon_{n,rms}$ versus Laser Injection Phase

7 Longitudinal Phase Space

When measuring the bunch length and energy spread of the electron bunch the timing of the RF system was adjusted such that the bunch was placed on the crest of the RF in the two linacs sections. This was accomplished by setting the overall linac phase with respect to the laser injection phase, by means of the low level RF system and $\delta\phi$ between the two linac section by means of a high power RF phase shifter, such that the energy of the beam was 41.4 MeV as measured in the energy spectrometer. The dispersion is in the energy spectrometer is 5.4 $\frac{mm}{\%}$. The energy spread was estimated by measuring the beam size on a phosphor screen in the dispersion region. Figure 10 is a plot of the energy spread of the electron bunch as a function of the linacs phase difference.

Electron bunch length was measured by dephaseing the second linac section such that a linear energy chirp is produced along the bunch. This allows the bunch length to be correlated to the energy spread and using the technique discussed previously to measure the energy spread, the bunch length is measured as a function laser injection phase. Figure 11 is experimental verification of bunch compression in the 1.6 cell RF gun. Bunch compression in the 1.5 cell RF gun have been experimental demonstrated previously [11].

8 Conclusions

We have experimentally studied the six dimensional phase space of the electron beam that is produced by the BNL/SLAC/UCLA 1.6 cell S-band Photocathode RF gun. We have experimentally verified longitudinal bunch compression, electron bunch energy and transverse emittance as a function of injection phase,

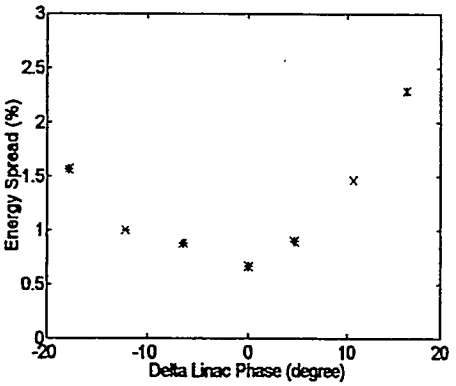

Figure 10: FWHM Energy Spread versus Linac Phase

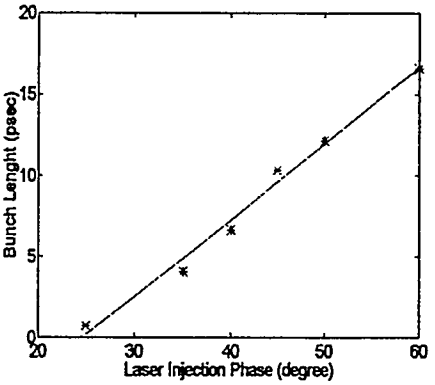

Figure 11: 95% Bunch Length versus Laser Injection Phase

solenoidal field and charge for peak fields in the RF gun of $127\frac{MV}{m}$. The optimized rms normalized emittance for a charge of 300 pC is 0.7 π mm mrad.

Future work includes multi-pole field studies that this gun is designed to suppress, cathode magnetic field effects, along with slice emittance and inverse RADON transforms that will elucidate the electron beams transverse phase space. Emittance measurements for a bunch charge of 1 nC are also planned.

9 Acknowledgments

The authors would like to thank the technical staff at the UCLA, Stanford Linear Accelerator Center and at Brookhaven National Laboratories Accelerator Test Facility for all their dedicated work on this project. We would also like to thank Mr. James N. Weaver from SSRL for all the technical discussions and help that he has provided the authors.

References

[1] B. E. Carlsten, *NIM*, **A285**, 313 (1989)

[2] K. Batchelor *et al.*, Proc. of 1990 EPAC p. 541

[3] D. T. Palmer *et al.*, Proc. 1995 Part. Accel. Conf. (1995) p. 982

[4] K. Halbach and R. F. Holsinger, *Particle Accelerators* **7**, 213 (1976)

[5] L. M. Young, private communications

[6] T. Srinivasan-Rao *et al.*, BNL-62626